Chemistry and Materials
The Center for Science Innovation

Research Article

Chem. Mater. 1 (3) 2022, 71-76

Green Synthesis of Nanoscale Zero-Valent Iron and Its Activity as an Adsorbent for Ni(II) and Cr(VI)

Novia Apriliani

Department of Chemistry, Faculty of Mathematics and Natural Sciences, Universitas Negeri Jakarta,
Jl. Rawamangun Muka, Jakarta 13220, Indonesia

*Corresponding author: noviaaprilianix@gmail.com

Received
18 July 2022
Received in revised form
27 October 2022
Accepted
29 October 2022
Published online
31 October 2022
DOI
https://doi.org/10.56425/cma.v1i3.29

Abstract

Zero-valent iron nanoparticles (nZVI) were successfully synthesized by metal salt reduction method using cinnamon as a reductor agent. Particle size analysis showed that the most optimum composition of $FeSO_4$ and polyphenols was at a ratio of 4:1, resulting in Dv(10), Dv(50), and Dv(90) values of 23.7 nm, 44.6 nm, and 178 nm, respectively. Scanning electron microscopy showed that nZVI was spherical and agglomerated. X-ray diffraction pattern showed a peak at 45.03° that corresponds to nZVI. The batch test showed that nZVI has Ni(II) and Cr(VI) adsorption activity of 95.58% Ni and 64.29%, respectively.

Keywords: zero-valent iron nanoparticles, polyphenols, cinnamon, adsorption, Ni(II), Cr(VI)

1. Introduction

Nowadays the increase in environmental pollution due to industrial waste containing heavy metals is one of the main concerns of the world [1]. Various attempts have been made to remediate heavy metal contaminants, both in soil and groundwater [2]. Adsorption technology is considered one of the most effective methods for removing heavy metals in water because it is easy to design and implement. Adsorption processes with various adsorbents such as activated carbon, graphene, alumina, zeolites, resins, microorganisms, and nano-zero valent iron (nZVI) have been studied extensively by researchers around the world. Among these adsorbents, nZVI is attractive due to its large surface area and high heavy metal adsorption capacity. Previous work showed that nZVI can be effectively used to remediate the environment from various contaminants, such as organic halogens, heavy metal ions, perchlorate, and nitrate [3].

Recently, various methods have been used to prepare iron nanoparticles. The most common method is by reacting iron salts with sodium borohydride [4]. However, this method has some limitations related to the toxicity of sodium borohydride, which may result in the production of flammable hydrogen gas during the synthesis process [5]. In addition, the tendency to form large agglomerates in a short time causes the reactivity and stability of nanoparticles to be reduced [6]. It is known that several plant extracts have potential as reducing agents and can be used to prepare iron nanoparticles with stable dispersions [7,8]. The method for synthesizing nanoparticles from plant extract is known as green synthesis. This method has many advantages, such as being eco-friendly, low-cost, and the obtained product is non-toxic. The active substances in plant extracts are polyphenol compounds, which are known as strong reducing agents and effective metal chelators. It can form stable complexes with iron [9] and also act as capping agents that prevents agglomeration of nanoparticles [10].

Based on previous work, nZVI has been successfully synthesized by green chemistry method using polyphenol reductant derived from kepok banana peel extract [11]. However, the difficulty of separating banana peel makes the polyphenols obtained not optimal and contain a lot of impurities. For this reason, another reductant was chosen from cinnamon that contains 131.34 mg g^{-1} of polyphenols [12]. From these results, it is estimated that cinnamon extract can be utilized as a reducing agent in the synthesis of iron nanoparticles. The synthesis of nZVI is affected by several factors, such as pH, reaction time, temperature, and precursor composition. This work is focused on determining the effect of the precursor composition ratio, namely $FeSO_4$ and polyphenol, on the preparation of nZVI particles. Furthermore, the adsorption test of the synthesized nZVI was carried out on nickel and chromium metals.

2. Materials and Method

The materials used during this work were *Cinnamomum burmanii* (Badan Penelitian Tanaman Obat dan Aromatik, Bogor, Indonesia), $FeSO_4$, NaOH, H_2SO_4, $NiSO_4.6H_2O$, and $K_2Cr_2O_7$ purchased from Merck. All the materials used were prepared in distilled water. First, 2 grams of fresh cinnamon that has been cut into small pieces is heated for 2 hours in 25 mL of water at 50˚C while stirring. After that, the extracted sample was filtered and the filtrate was diluted to a volume of 25 mL. Then, this filtrate is stored in the refrigerator. The synthesis of nZVI was carried out by mixing polyphenols from cinnamon extract with $FeSO_4$ at composition ratio of 2.5:2.5, 3:2, and 4:1. After that, the solution was stirred at 200 rpm for 60 minutes. Finally, the nZVI formed was filtered with Whatman paper No. 40.

The filtrate obtained was characterized by a particle size analyzer (PSA, Dynamic Light Scattering: Zetasizer Nano ZSP) to determine the size distribution of the nZVI particles formed. In addition, the filtrate was also dried using the freeze-dry method before being characterized using Fourier transform infrared spectroscopy (FTIR, IR Prestige-21 SHIMADZU), energy dispersive X-ray spectroscopy connected to scanning electron microscopy (SEM-EDX, JEOL JSM 651-OLA), X-ray diffraction (XRD), and atomic absorption spectroscopy (AAS).

The adsorption test was carried out using the batch method by reacting 20 mL of $NiSO_4.6H_2O$ 10 mg L^{-1} and 20 mL $K_2Cr_2O_7$ 7 mg L^{-1} with 0.1 g of nZVI, respectively. For Ni(II) adsorption, the solution pH was adjusted to 8 by adding NaOH. While for Cr(VI) adsorption, the solution pH was adjusted to 3 by adding H_2SO_4. All ingredients were then shaken at 150 rpm at room temperature for an hour, 5 hours, 10 hours, 15 hours, and 20 hours. Finally, the filtrate was filtered using Whatman paper No. 40 to measure the remaining Ni(II) and Cr(VI) levels with AAS.

3. Results and Discussion

The FTIR spectra of polyphenols extracted from cinnamon are shown in Fig. 1. Based on this spectrum, a peak at 3346.50 cm^{-1} indicates the presence of a hydroxyl group (O-H) [13]. A peak at 2943.37 cm^{-1} corresponds to stretching C-H alkane. Peaks at 1608.63 cm^{-1} and 1523.76 cm^{-1} show the absorption area of the aromatic C=C functional group due to the vibration of the aromatic compound. A peak at 1448.54 cm^{-1} indicates a bending characteristic of C-OH alcohol. A peak at 1284.59 cm^{-1} is related to $–CH_2$ alkane which swings and aromatic ring =C-H for bending absorption in the plane. A peak at 1062.78 cm^{-1} characterize the absorption area for C-O alcohol which is a substituent of the hydroxyl group on the benzene ring caused by the deformation vibration of C-OH [14]. A peak at 819.75 cm^{-1} indicates the presence of substituted aromatic compounds. A peak at 705.95 cm^{-1} – 779.24 cm^{-1} and 628.79 cm^{-1} are due to the absorption of C-H in the benzene ring and alkene, respectively. This data confirmed that the sample obtained is phenolic.

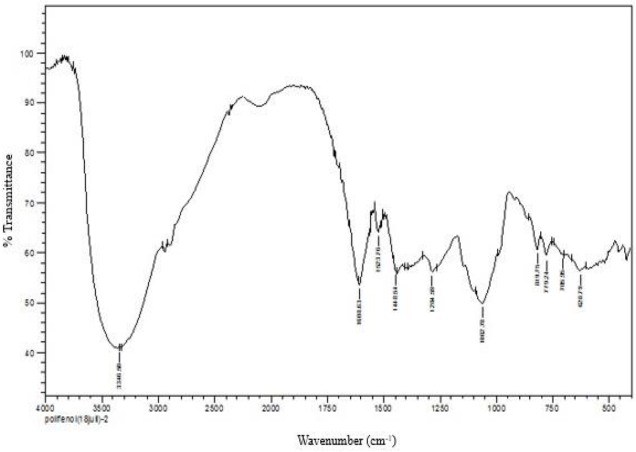

Figure 1. FTIR spectra of polyphenols

PSA characterization in Fig. 2 shows that ZVI obtained from the ratio of polyphenols and $FeSO_4$ 4:1 is the most optimum composition. At this composition, Dv(10), Dv(50), and Dv(90) were 23.7 nm, 44.6 nm, and 178 nm, respectively. This result is quite different when compared to the composition of another sample with a different composition ratio. The chemical reduction method in the synthesis of nanoparticles contains four steps, including (1) saturation of the solution, (2) nucleation of the nZVI cluster, (3) nZVI core growth, and (4) nZVI agglomeration. From this work, at nZVI 4:1 the amount of polyphenols used is sufficient to reduce Fe^{2+} to Fe^0, which is then capped very well by polyphenols, resulting in smaller particles. This can be seen from the values of Dv(10), Dv(50), and Dv(90) which resulted in the lowest particle size distribution compared to other composition samples. This nZVI also produces a polydispersity index (PDI) with a low value of 0.442.

At nZVI 2.5:2.5 and 3:2, the number of polyphenols used was not enough to cap the resulting nanoparticles. As a result, agglomeration happened which causes the formation of larger particle sizes. This is evidenced by the values of Dv(10), Dv(50), and Dv(90) which are 80.3, 1300, and 2040 nm for nZVI 3:2. While for nZVI 2.5:2.5 was 1440, 1960, and 2630 nm.

Table 1. Particle size distribution of nZVI

Cumulative Method	Composition ratio between polyphenols and $FeSO_4$		
	2.5 : 2.5	3 : 2	4 : 1
Dv10 (nm)	1440	80.3	23.7
Dv50 (nm)	1960	1300	44.6
Dv90 (nm)	2630	2040	178
PDI	0.313	0.462	0.442

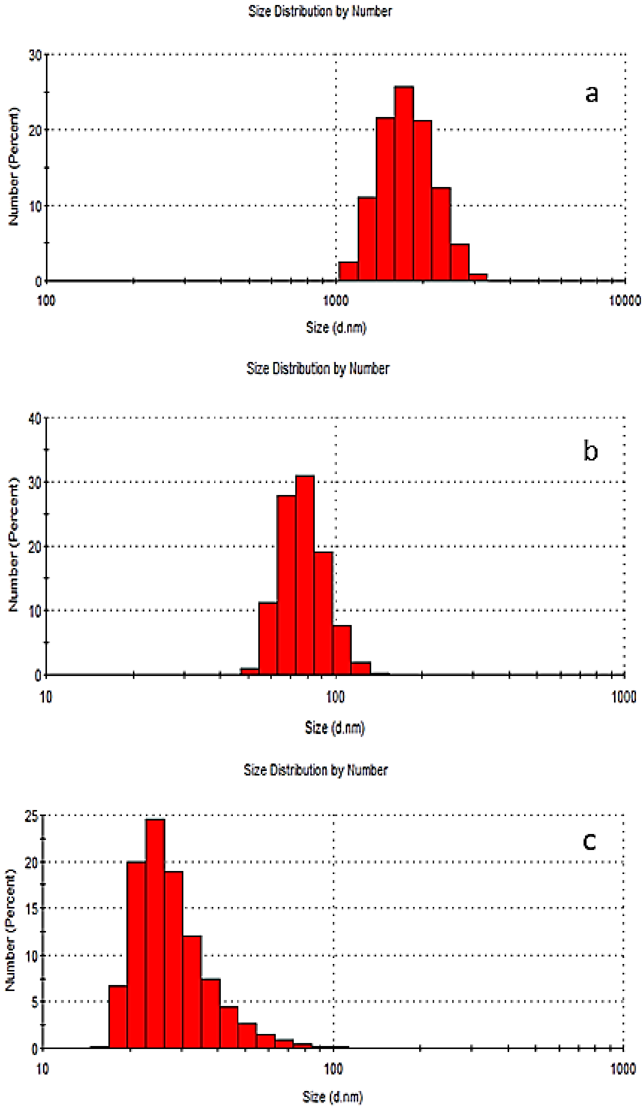

Figure 2. Particle size distribution of nZVI synthesized at different composition of polyphenol and $FeSO_4$: a) 2.5:2.5 b) 3:2 c) 4:1

The FTIR spectrum of nZVI 4:1 is shown in Fig. 3. Based on this result, there are several different peaks when compared to the FTIR spectrum of polyphenols. This difference indicates a change in the structure of the functional group from polyphenols to nZVI. A peak at 3390.86 cm^{-1} indicates stretching O-H. A peak at 1604.77 cm^{-1} related to the absorption of the aromatic C=C functional group. A peak at 1093.64 cm^{-1} according to the presence of inorganic SO_4^{2-} [16] derived from $FeSO_4$. While peaks at 443.63, 511.14, and 619.5 cm^{-1} indicate the presence of Fe-O bonds from Fe_3O_4 and Fe_2O_3, respectively. At these wavenumbers, stretching of Fe-O occurs from the tetrahedral and octahedral sides in its structure [17,18]. The formation of Fe-O is because nZVI has been oxidized to iron oxide.

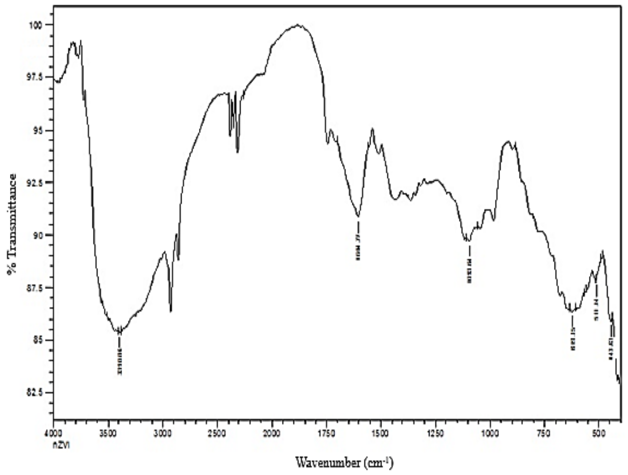

Figure 3. FTIR spectra of nZVI

Fig. 4 shows the nZVI morphology of polyphenols and $FeSO_4$ in a ratio of 4:1. From the micrograph, it is known that nZVI has a spherical shape and inhomogeneous. Nanoparticles have large specific surfaces and high surface energies. Therefore, nanoparticles tend to agglomerate. Nanoparticle agglomeration can occur due to interparticle interactions, such as Van der Waals forces and magnetic interactions [19].

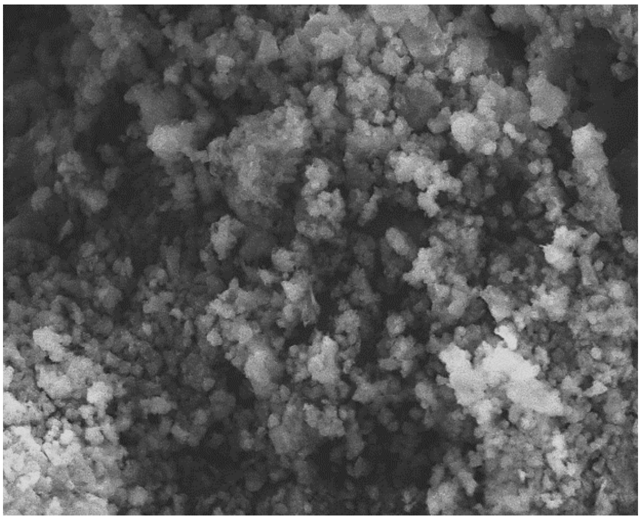

Figure 4. Micrograph of nZVI

The synthesized nZVI was also characterized using EDX. The result is shown in Fig. 5. Based on EDX data, nZVI 4:1 has 5.71% Fe components and 45.09% oxygen. The large mass percentage in nZVI indicates that oxidation has occurred which continues at the corrosion stage. This iron corrosion reaction will be used for water remediation from various kinds of contaminants, both organic and inorganic [20]. In addition, there are also S atoms derived from $FeSO_4$ residue which may come from filter paper made of cellulose or carbon tape used during SEM analysis. The K atom in the spectrum is thought to be an impurity.

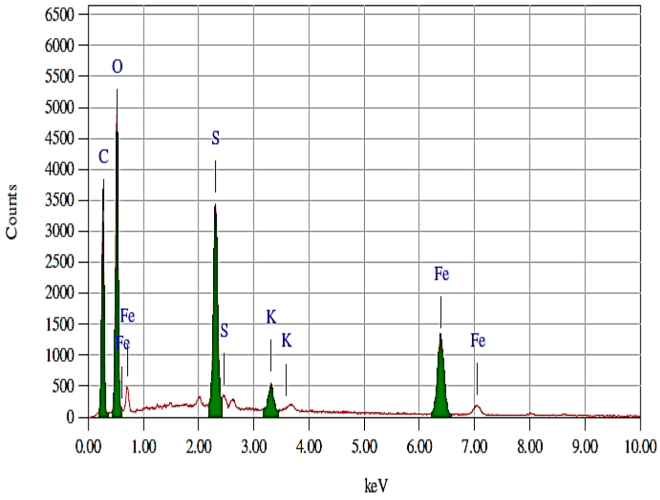

Figure 5. EDX spectrum of nZVI

The results of the XRD analysis are shown in Fig. 6. It is known that the nZVI crystalline phase is at the peak of 2θ 45.03^0 [21]. While the hematite phase (Fe_2O_3) is at the peak of 2θ = 34.48^0 and 49.39^0. The presence of these two phases was because nZVI had been oxidized to its iron oxide.

The effectiveness of Ni^{2+} and Cr^{6+} metal removal by nZVI will be demonstrated using a batch test. The percentage of Ni and Cr adsorbed can be calculated using Eq. 1 [22].

$$\% \text{ Adsorption} = \frac{(C_0 - C_e)}{C_0} \times 100 \qquad (1)$$

where C_0 and C_e are the initial and final metal ion concentrations (mg L^{-1}), respectively.

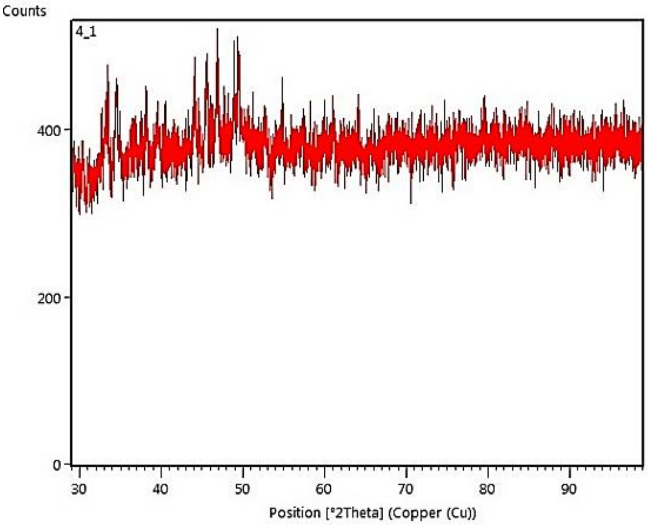

Figure 6. Diffractogram pattern of nZVI

The results of the nickel adsorption test using nZVI are shown in Fig. 7. Based on this curve, it can be seen that in the first hour, the percentage of Ni(II) and Cr(VI) adsorption reached 76.46% and 56.21%, respectively. The percentage of Ni(II) adsorption then increased significantly up to 95.58% at 5 hours [23]. Meanwhile, in the Cr(VI) adsorption test, the highest adsorption percentage was 64.29% which was achieved within 10 hours. Adsorption tends to increase to the optimum point and then decrease with increasing contact time. This is because the active site has been saturated due to bonding with metal ions and an equilibrium between the adsorbate and adsorbent has been reached.

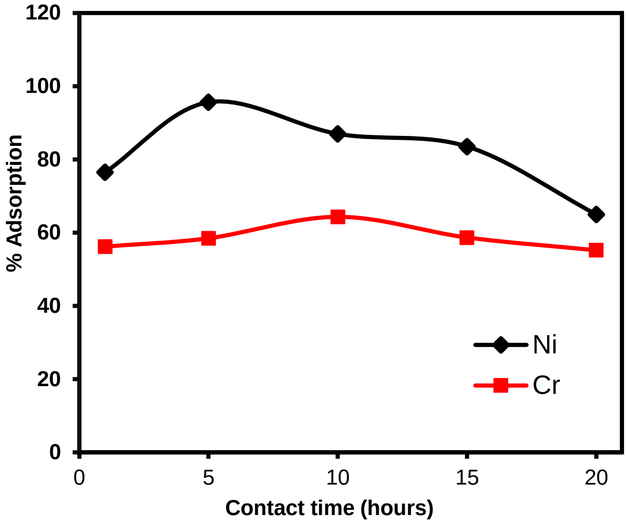

Figure 7. The relationship between contact time and percentage of metal adsorption

Fig. 8 shows the comparison of the FTIR spectra before (red line) and after adsorption (black line) with nZVI. There are new peaks that appear in the 430 cm^{-1} and in the range of 1200 cm^{-1} – 1400 cm^{-1} which indicate the presence of Ni-O bonds [25].

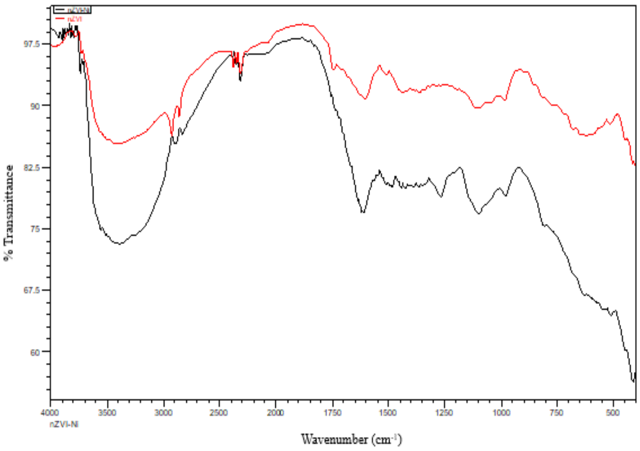

Figure 8. Spectra of nZVI before (red line) and after adsorption (black line)

4. Conclusions

The nZVI has been successfully synthesized from $FeSO_4$ using natural reducing agents, namely polyphenols derived from the cinnamon extract. The results of the size and distribution analysis using PSA showed that the optimum composition ratio of $FeSO_4$ and polyphenols was 4:1 with values of Dv(10), Dv(50) and Dv(90) 23.7 nm, 44.6 nm, and 178 nm, respectively. SEM shows that the surface of nZVI is spherical and inhomogeneous. Based on the metal adsorption test, nZVI can be used to adsorb Ni(II) and Cr(VI) with removal percentages reaching 95.58% and 64.29% with an optimum time of 5 and 10 hours, respectively.

Acknowledgement

The authors thank Direktorat Pendidikan Tinggi for supporting this work under Hibah Bersaing Scheme 2015.

References

[1] Ghaedi, M., Hajjati, S., Mahmudi, Z., Tyagi, I., Agarwal, S., Maity, A., Gupta, V.K., Modeling of competitve ultrasonic assisted removal of the dyes-methylene blue and safranin-O using Fe_3O_4 nanoparticles, *Chemical Engineering Journal*. (2015) 268:28–37.

[2] Rickerby, D.G. & Morrison, M., Nanotechnology and the environment: a European perspective, *Science and Technology of Advanced Material*. (2007) 19–24.

[3] Yaacob, W., Kamaruzaman, N., Rahim, A., Development of nano-zero valent iron for the remediation of contaminated water, *Chemical Engineering Transaction.* (2012) 28:25–30.

[4] Wang, T., Su, J., Jin, X., Chen, Z., Megharaj, M., Naidu, R., Functional clay supported bimetallic nZVI/Pd nanoparticles used for removal of methyl orange from aqueous solution, *Journal of Hazardous Materials*. (2013) 262.

[5] Li, X.Q., Elliott, D.W., W-Q, Z., Zero-valent iron nanoparticles for abatement of environmental pollutants: materials and engineering aspects, *Critical Reviews in Solid State and Material Science.* (2006) 31:111–122.

[6] Chen, Z., Wang, T., Jin, X., Chen, Z., Megharaj, M., Naidu, R., Multifunctional kaolinite-supported nanoscale zero-valent iron used for the adsorption and degradation of crystal violet in aqueous solution, *Advance in Colloid and Interface Science*. (2013) 398.

[7] Hoag, G., Collins, J., Holcomb, J., Hoag, J., Nadagouda, M., Varm, R., Degradation of bromothylmol blue by 'greener' nano-scale zero-valent iron synthesized using tea polyphenols, *Journal of Material Chemistry*. (2009) 19.

[8] Shahwan, T., Abu Sirriah, S., Nairat, M., Eroglu, A., Scott, T., & Hallam, K., Green Synthesis of Iron Nanoparticles and Their Application as a Fenton-Like Catalyst for the Degradation of Aqueous Cationic and Anionic Dyes, *Chemical Engineering Journal*. (2011) 172:258-266.

[9] Perron, N.R. & Brumaghim, J.L., A Review of the Antioxidant Mechanisms of Polyphenol Compounds Related to Iron Binding, *Cell Biochem Biophys*. (2009) 53:75.

[10] Njagi, E.C., Huang, H., Stafford, L., Genuino, H., Galindo, H.M., Hoag, G.E., Biosynthesis of iron and silver nanoparticles at room temperature using aqueous Sorghum Bran extracts, *Langmuir*. (2010) 27.

[11] Pribadi, G.A., Pengaruh Waktu Reaksi dalam Sintesis Besi Bervalensi Nol (ZVI) dari $FeSO_4$ dengan Ekstrak Polifenol Kulit Pisang Kepok, *Jurnal Riset Sains dan Kimia Terapan*. (2014) 4(2)398-404.

[12] Nely, Fany, Aktivitas Antioksidan Rempah Pasar dan Bubuk Rempah Pabrik dengan Metode Polifenol dan Uji AOM (Active Oxygen Method), IPB. (2007).

[13] Adinew, Bizuneh, GC-MS and FT-IR analysis of constituents of essential oil from Cinnamon bark growing in South-west of Ethiopia, *International Journal of Herbal Medicine*. (2014) 1(6), 22-31.

[14] Li, Y.Q., Kong, D.X., Wu, H., Analysis and evaluation of essential oil components of cinnamon barks using GC–MS and FTIR spectroscopy, *Industrial Crops and Product*. (2013) 41:269- 278.

[15] Seabra, A.B., Haddad, P., Duran, N., Biogenic synthesis of nanostructured iron compounds: applications and perspectives. *IET Nanobiotechnology*. (2013) 7(3), 90–99.

[16] Nakamoto, Kazuo, Infrared and Raman Spectra of Inorganic and Coordination Compounds Sixth Edition. John Wiley & Sons, Inc., Hoboken, New Jersey. (2009).

[17] Zhang, X., Lin, S., Chen, Z., Megharaj, M., Naidu, R., Kaolinite-supported nanoscale zero-valent iron for removal of Pb^{2+} from aqueous solution: Reactivity, characterization and mechanism, *Water Research.* (2011) (45):3481-3488.

[18] Baikousi, M., Bourlinos, A.B., Douvalis, A., Bakas, T., Tuček, J., Šafářová, K., Zboril, R., Synthesis and Characterization of γ-Fe_2O_3/Carbon Hybrids and Their Application in Removal of Hexavalent Chromium Ions from Aqueous Solutions, *Langmuir*. (2012) 28:3918–3930.

[19] Zare, Yasser. Study of nanoparticles aggregation/agglomeration in polymer particulate nanocomposites by mechanical properties, *Composites: Part A*. (2016) 84:158-164.

[20] O'Hannesin, S.F., & R.W. Gillham, Long-term performance of an in situ "iron wall" for remediation of VOCs, *Ground Water*. (1998) 36(1)164–170.

[21] Nurmi, J.T., Tratnyek, P.G., Sarathy, V., Baer, D.R., Characterization and properties of metallic iron

nanoparticles: Spectroscopy, electrochemistry, and kinetics. Environmental Science and Technology. (2005) 39: 1221–1230.

[22] Ravindra, K. M., Banerjee, S., Sanjeev, K., Chandra, M, Removal of Ni(II) by magnetic nanoparticles, *Journal of Molecular Liquids*. (2015).

[23] Efecan, N., Shahwan, T., Eroğlu, A., Lieberwirth, I., Characterization of the uptake of aqueous Ni^{2+} ions on nanoparticles of zero-valent iron (nZVI), Desalination. (2009) 249:1048–1054.

[24] Rajasekhar, K & Saritha, B., Equilibrium Studies of Malachite Green from Aqueous Solution Using Corn Cob as Adsorbent, *International Journal of Engineering Research and Development*. (2014) 10(11):41-48.

[25] Adekunle, A.S., Oluwafemi, O.S., Ogunfowokan, A.O., Eleruja, M.A., Comparative Catalytic Properties of $Ni(OH)_2$ and NiO Nanoparticles Towards the Degradation of Nitrite (NO^{2-}) and Nitric Oxide (NO), *International Journal of Electrochemical Science*. (2014) 9:3008-3021.